FACULTY OF SCIENCES

Study on genes involved in Alzheimer's Disease

Analysis on omics data using R

Bianca De Saedeleer
01409888

Faculty of Sciences
Master of Science in Bioinformatics – Bioscience Engineering
Applied High-Throughput Analysis
Prof. dr. ir. De Meyer
Academic year: 2018 – 2019

GHENT UNIVERSITY

Table of Contents

List of Abbreviations

Aβ	Amyloid-beta
AD	Alzheimer's Disease
APOE	Apolipo Protein E
APP	Amyloid Precursor Protein
CNS	Central Nervous System
DE	Differentially Expressed
DMCGs	Differentially Methylated CpGs
GSA	Gene Set Analysis
miRNAs	Micro RNAs
ncRNAs	Non-coding RNAs
ORA	Overrepresentation Enrichment Analysis
PSEN1	Presenilin-1
PSEN2	Presenilin-2
ROS	Reactive Oxygen Species
TF	Transcription Factor
TFBSs	Transcription Factor Binding Sites
TSSs	Transcription factor Start Sites
VDAC1	Voltage-Dependent Anion Channel 1

Part I: General information

Introduction about Alzheimer's Disease

In 2010, around 36 million people worldwide were suffering from dementia (ADI, 2013). Due to the higher age expectancy this number will be 75 million by 2030 and will probably increase to 135 million by 2050 (ADI, 2013), indicating the importance of finding treatments and ways for prevention. In 60% of the cases, dementia is caused by Alzheimer's disease (AD) which is a chronic neurodegenerative disorder leading to behavioural changes, loss of cognitive abilities and eventually death (Lunnon & Mill, 2013; Nativio et al., 2018). The most common form of AD is sporadic or late onset AD which is linked with the ε4 allele of the APOE (Roy & Bhattacharyya, 2016). The rare form is early onset familial AD, mainly caused by mutations in the APP, PSEN1 and PSEN2 genes leading to the accumulation of amyloid-β (Aβ) protein causing functional and structural brain alterations such as amyloid plaques. Hyperphosphorylation of the microtubule-associated tau protein is also recognized to be causal contributing in the formation of neurofibrillary tangles and destabilization of the skeletal structure of the neurons leading to degeneration (Balez & Ooi, 2015; Lau et al.,2013; Lunnon & Mill, 2013; Roy & Bhattacharyya, 2016; Sperling et al., 2011; Nativio et al., 2018). Other known symptoms of AD due to Aβ deposition and elevated APP production are increased ROS production, impaired mitochondrial activity (mitochondrial dysfunction), decreased neural ATP production, inflammation, synaptic oxidative stress, free radical production and reduced cerebral glucose utilization (Cisternas & Inestrosa, 2017; Manczak & Reddy, 2013).

Brain regions responsible for cognition are more prone to these plaques and tangles (Sperling et al., 2011). The degree of spreading of plaques and tangles (based on the detectable presence of the hyperphosphorylated tau protein) across the brain regions is used as a classification measure for AD, i.e. Braak stages (Braak et al., 2006). Braak stages are divided into 6 stages depending on the affected regions (Table 1 and Figure 1, Supplementary). More knowledge about the epigenetic variation and underlying molecular causes, such as DNA and histone modifications, and its correlation with aging, gender and tissue specificity is needed (Gasparoni et al., 2018; Lunnon & Mill, 2013).

Objective

The aim of this study is to investigate the genes, the related pathways and the biological processes involved in AD pathogenesis by humans. This will be done by investigating the methylation differences in the frontal cortex (post-mortem tissue) of AD patients and healthy people. The obtained results imply that non-coding RNAs (ncRNAs) might be involved, therefore a RNA-seq dataset about the alteration of ncRNAs in the prefrontal cortex during the progression of AD, is studied.

Material and Methods

Dataset 1: GSE66351 - Methylation profiling by array

In this analysis bulk samples derived from post-mortem tissue of the human frontal cortex are studied. The aim is to determine the samples with differentially methylated CpGs (DMCGs) and to identify the associated genes on a significance level of 0.05 for the adjusted p-values. The selected samples are part of a bigger dataset of 128 Caucasian samples obtained by methylation profiling using Illumina's HumanMethylation 450k bead array from a study by Gasparoni et al. (2018). DNA methylation modifications in glial and neuronal cells associated with aging and AD progression are searched for. The goal of the original article is to report differences in the DNA methylation of the human brain correlated with aging and/or increasing Braak stages. To gain more discriminative power and reduce confounding noise due to variable cell composition, cell-type purification is performed. The data can be found at the NCBI GEO database under GSE66351.

Analysis

The distribution of the samples is unbalanced, therefore, random sampling will be performed in order to get equal groups. The group of healthy women has the least number of samples (10), for each group, 10 samples are randomly taken. Bad quality data is removed, quantile normalization is performed using the wateRmelon package (Pidsely et al.,2013). Quality control and data exploration is done by checking MDS-, volcano- and MA-plots. The Limma package (Ritchie et al., 2015) is used for the statistical analysis and empirical Bayes moderation is applied because of the small sample size (20 vs 20). The final results are listed in Table 2 and Table 3 (Supplementary). For further reasoning behind the used methods, interpretation of the plots and details of the analysis, the reader is referred to AnalysisFC_HM450k.pdf.

In order to get a better overview of the most important pathways that are involved, gene set analysis (GSA) is performed using limma. All the adjusted p-values of the pathways turn out to be 1, the Benjamini-Hochberg correction that is applied for testing 1506 genes, could be the cause. Because of the high number of considered genes, the correction will also be higher, resulting in 1's. Visualization of the involved pathways is obtained by the online Webgestalt (2017) tool (Wang et al. 2017) (Figures 2 and 3, Supplementary).

Dataset 2: GSE48552 - Non-coding RNA profiling by high throughput sequencing

Lau et al. (2013) perform a high-throughput profiling for 2038 different miRNAs from 12 samples of post-mortem tissue of the prefrontal cortex of patients (Homo sapiens) grouped by Braak stages (6 early vs 6 late), using the Illumina HiSeq 2000. miRNAs are ncRNAs of 22 nucleotides long that control genes by translational inhibition or transcriptional repression through binding to transcripts of particular genes or mRNA degradation that contribute in physiological and pathological signaling pathways (Lau et al., 2013; Roy & Bhattacharyya, 2016). The objective is to study the miRNA expression alterations during the progression of AD. The raw data is available in SRA under the accession SRP026562. The NCBI GEO database provides the raw and normalized counts under accession GSE48552.

Analysis

As a quality control and since the authors do not provide an overview of the basic characteristics, is preprocessing of one sample is executed on the Porthos server of UGent. The fastqc file shows that the data is of moderate quality, for a detailed discussion on it, the reader is referred to QC_ncRNAs.pdf. The basic characteristics are displayed in Table 4 (Supplementary). Due to limited memory available on the server, the accessible raw counts from the authors are used. A short overview of the handled pipeline is written down in Analysis_ncRNAs.pdf.

In the filtering step, low counts (<30, same threshold as the authors) are removed since they won't result in significant results and will influence the results, trend and FDR calculation incorrectly, also the log fold changes are not reliable for low counts. Since only 12 samples are available, EdgeR (McCarthy et al., 2012; Robinson et al., 2010) is used for statistical testing instead of the more conservative DESeq (De Meyer, 2018), TMM normalization is performed. Differences in library size are detected and corrected for. Quality control, data exploration is done by looking at the MDS-, BCV-, MA- and goodness of fit plots, showing overfitting, lack of fit and overall no distinct differentialy expressed (DE) loci. Also the distribution of the p-values is visualized which indicates unreliable results. All 546 miRNAs are down regulated and significantly DE, which doesn't seem trustworthy. A possible explanation is a batch effect between the samples of the early and late stage, proven in Analysis_ncRNAs.pdf. Because of the unreliable results, the statistical analysis is repeated applying DESeq2, however, here no significant results are obtained, indicating lack of power (6 vs 6) and that DESeq2 is too conservative for this dataset. Finally, voom-limma (Law et al., 2014) is used where empirical Bayes moderation is carried out due to the small sample size. This results in 534 significantly DE miRNAs. For further reasoning behind the used methods, interpretation of the plots and details of the analysis, the reader is referred to Analysis_ncRNAs.pdf.

The comparison of edgeR, DESeq2 and Voom Limma illustrates that edgeR is too liberal whereas DESeq2 is too conservative in this particular context. Voom seems to be a fair compromise that can handle differences

in sequencing depth better and is able to control the type I error rate accurately for small sample sizes (Law et al., 2014).

To get insight into the involved pathways, GSA using limma is performed. Again resulting is adjusted p-values of 1, due to high BH correction and lack of power since this analysis is a 6 vs 6.

Results and Discussion

Dataset 1: GSE66351 - Methylation profiling by array

Table 8 (Supplementary) displays the functions of a selection (arbitrary chosen) of genes within a 2500 bp distance from the obtained significant probes. It shows that genes with different functions are involved in DMCGs. Several genes contribute to brain and CNS development such as SH3GL3, NDN, PPP3CC, WNT2, ANKLE2, ARSB, JRKL, POTEE and NAGLU. The transcription factor of the TFCP2 gene activates the alpha-globin gene which polymorphisms play a role in the pathogenesis of Alzheimer's disease. CFAP70 and DNAH17 play a role in the mobility of cells; ANKLE2, CYFIP2, SRF and TPX2 influence apoptosis; CGGBP1, N4BP2L2, MIER3, MIR4255 and USP3 regulate transcription negatively and SRF, TFCP2, TOX2, ZBTB17 and ZFP30 regulate transcription positively. Also ncRNAs such as JRKL-AS1 and MIR4225 and uncharacterized ones such as LOC285889 and LOC646903 might be involved in the appearance of AD. The output of the GSA in R and by the Webgestalt tool confirms the previously stated findings, a selection of the results is listed in Table 5 (Supplementary). The obtained genes are mainly involved in glycosaminoglycan degradation, apoptosis, cell cycle, pathways in cancer, the fructose and mannose metabolism and the metabolism of selenium which has a protective function against several cancers (Ip, 1998). The main involved biological processes (Figure 2 and 3, Supplementary) are differentiation and regulation of neurogenesis, regulation of nervous system development, trophectodermal cell differentiation, RNA, mRNA, tRNA and ncRNA processing and the positive regulation of nitrogen compound metabolic process. The latter is known to induce nitrotyrosination of proteins leading to oxidative stress and accumulation of proteins and therefore contributing to the progression of neurodegenerative processes (Guix et al., 2009; Huang et al., 2016; Picón-Pagès et al., 2018). Since a majority of the involved pathways corresponds to the ones obtained for the dataset of ncRNAs, further discussion is given in the following section.

Some obtained genes are linked to other diseases:

- The product of GNS is a lysosomal enzyme that hydrolyzes the 6-sulfate groups of the N-acetyl-D-glucosamine 6-sulfate units of heparin, heparan sulfate and keratan sulfate (UniProtKB P15586, 2018). Accumulation of these compounds can lead to the Sanfilippo D syndrome. Another gene that is involved is the catabolism of heparan sulfate is NAGLU. Sanfilippo B syndrome causes malfunctioning of this gene, leading to neurodegradation, behavioral changes and a shortened lifespan (NCBI MedGen, 2018), which are also symptoms of AD.
- NUB1 encodes a negative regulator of NEDD8, which accumulate in Lewy bodies in Parkinson's disease and dementia. It also encodes for proteins that respond to tumor necrosis factors (NCBI Gene NUB1, 2018).

The obtained results of this analysis point to possible interesting genes that might be involved in AD and shouldn't be literally interpreted as the truth. The consequences of hyper- and hypomethylation depend on each gene individually and need further investigation since genes involved in the same pathway show different degrees of methylation. Following genes are hypermethylated: ABLIM2, CYFIP2, ESYT2 , GNS, GPD2 , HSP90AA1 , LFNG, MIER3, SERINC2 , SRF and ZFP30 which have very different functions (Table 2, Supplementary). Hypomethylated genes (62) are listed in Table 3 (Supplementary).

Comparison with the original article: Gasparoni et al. (2018)

The MBP gene which is involved in signaling pathways in T-cells and neural cells, is also reported by Gasparoni et al. (2018). Besides that, the majority of the obtained significant genes don't correspond to the ones found in the original study. A possible explanation is that the authors use multiple linear regression models to correct for sex, age and technical batch effects. Also, frontal cortex and temporal cortex samples are separately evaluated to eliminate brain region effects. In this analysis, only the gender effect is taken into account with an additive linear model since the aim of this task is to understand the reasoning behind the analysis and not necessarily performing an extensive research. Furthermore, proving the significance of interaction terms asks more power which is difficult for small sample sizes and it often complicates the interpretability. Gasparoni et al. (2018) mention as additional explanation that DNA methylation at cytosines and the level of heterogeneity in cell-type composition can differ between populations as well as in individuals, resulting in lower detection power. In addition, Hokama et al. (2013) show in their study that the expression levels in genes from the frontal cortex alter less than genes in the hippocampi and temporal cortex which can result in less possibility to detect those genes as significantly affected ones. Furtheron, differences in used functions, packages and the chosen significance level can also lead to variation in the found differentially methylated genes. For example, the preprocessing steps differ: the authors perform quantile normalization and background subtraction using the minfi package, as well as batch effect correction using Combat from the sva package. Probes with a p-value above 0.01 are removed.

Despite the non-corresponding addressed genes, the involved pathways found with GSA do agree (Supplementary Table S19 of Gasparoni et al., 2018). Important to mention is that Gasparoni et al. (2018) detect a limited number of epigenetic markers in the bulk samples which do not correspond with other EWAS studies due to lack of discriminative power and a smaller cohort. This implies that further research is needed.

Dataset 2: GSE48552 - Non-coding RNA profiling by high throughput sequencing

A part of the obtained biological processes and pathways in the GSA are shown in Table 6 and 7 (Supplementary), respectively. According to the achieved results, DE miRNAs seem to be involved in many diverse pathways similar to the ones found for the DMCGs dataset (Table 5, Supplementary) implying a link between DMCGs and miRNAs. Considering the large amount of involved pathways and the page restriction of this work, a small selection will be discussed.

DNA methylation mainly occurs in CpG islands laying upstream promoter regions of genes. Methylated TFBSs or TSSs will influence the TF regulation which will hinder the transcription of the downstream miRNAs and genes therefore interfering with the gene expression and silencing and thereby introducing disease phenotypes. If the affected miRNAs are participating in pathways within the CNS like the development, differentiation and synaptic plasticity of neuronal cells, accumulation of Aβ42 oligomers will occur, inducing neurodegenerative diseases such as AD and Parkinson's disease because this deposition causes lowered glucose consumption and mitochondrial activity in brain regions (hippocampus and cortex) that provide cognitive functions (Cisternas & Inestrosa, 2017; Roy & Bhattacharyya, 2016; Zendjabil, 2016). Gene silencing is a recurrent pathway in the outcome of the executed GSA, silencing of the APP, Tau and VDAC1 genes could recover synaptic and mitochondrial activity and reduce Aβ aggregation , since these genes are acknowledged to be toxic for AD neurons (Manczak & Reddy, 2013).

Additionaly, metabolic energy pathways appear to be highly affected in AD pathogenesis based on the obtained involved processes of this analysis. This is also proven in literature. The main energy source of the brain is glucose (25% of the total body glucose) with neurons using 70% of it. Glucose uptake and intracellular oxidative metabolism are the two stages of the glucose metabolism which seem to be connected to molecular alterations such as down regulated expression of the glucose transporters GLUT1, GLUT3 and GLUT4 in the cortex and hippocampus, insulin resistance in the brain, mitochondrial dysfunction, deregulation of the Krebs cycle and oxidative phosphorylation. Wnt signaling would be involved as a metabolic regulator and

would be crucial for the development and function of the CNS and mitochondria (Figure 4, Supplementary) (Cisternas & Inestrosa, 2017; Yin et al., 2016).
Another metabolic regulator in the reduction of the mitochondrial energy production, the pentose-phosphate pathway and the glycolytic pathway (with GLUT1 and GLUT3 being involved) is nitric oxide (Bolaños et al., 2008). This finding can be associated to the positive regulation of nitrogen compound metabolic process found for the DMCGs dataset.
A recurrent link between the miRNA and methylation dataset is the pathways and processes involved in diabetes, insulin signaling, stimulus and secretion. Several studies and review articles investigate this connection (Baglietto-Vargas et al., 2016; Hokama et al., 2013). Besides, cancer-related signaling pathways (Figure 5, Supplementary) such as the mTOR-, HIF- and MAPK-pathway are found in both datasets and are as well acknowledged to have a correlation with AD, ageing and mitochondrial dysfunction, but the exact role they are playing is not unraveled yet (Guo et al., 2017; Zendjabil, 2018).

Comparison with the original article: Lau et al. (2013)

Lau et al. (2013) have found 41 deregulated miRNAs and stress the strong alteration in miR-132-3p. At Braak stages III and IV miR-132-3p in neurons displaying tau-hyperphosphorylation are downregulated and show a decrease in quantity, before neuron-specific miRNAs loss itself. Related miRNAs in the same cluster on chromosome 17 are also lowered. miR-132-3p regulates mRNA targets in the tau network and the FOXO transcription factors, therefore influencing AD progression. FOXO proteins would carry out a protective function by repressing tumorigenesis, inducting apoptosis and would act as homeostatic regulators against stress (Guo et al., 2017).
miR-132-3p and connections with FOXO pathways are also found in the output of the executed analysis, but not as top results. A possible reason for this difference can be the use of voom instead of DESeq in combination with the small sample size. The authors also state that the overall cellular composition of the prefrontal cortex as well as the general expression profile of miRNAs stay more or less the same regardless of the Braak stages, which can results in low discriminative power. Furthermore, the same problem with the heterogeneity of the brain tissues as mentioned before, influences the results.

Conclusion

The involved genes, miRNAs and their role in the various pathways and metabolic processes obtained in this analysis illustrate the complexity of AD pathogenesis and explains why only limited medication is available, namely memantine and cholinesterase inhibitors that delay the symptoms of AD, but are not able to cure affected patients (Balez & Ooi, 2016; Sancesario & Bernardini, 2018). Therapies that tackle the accumulation of Aβ42 fail in treating or slowing down AD (Zendjabil, 2018). Zendjabil (2018) suggests to develop treatments targeting the downstream impact of silencing, with miRNAs being a possible agent. He proposes 3 potential approaches: miRNA mimics in cases of down regulation, anti-miRNAs for overexpression and molecules that can interact with miRNAs.
Sancesario and Bernardini propose a multi-omics approach (Figure 6) where results from different -omics technologies are combined to investigate the linkage between the different pathways in order to understand this complex biology and to get closer to a cure. This suggestion is also mentioned by Wang et al. (2019). The latter also give two comprehensive figures of the associated genes and miRNAs in AD pathogenesis (Figure 7 and 8, Supplementary).

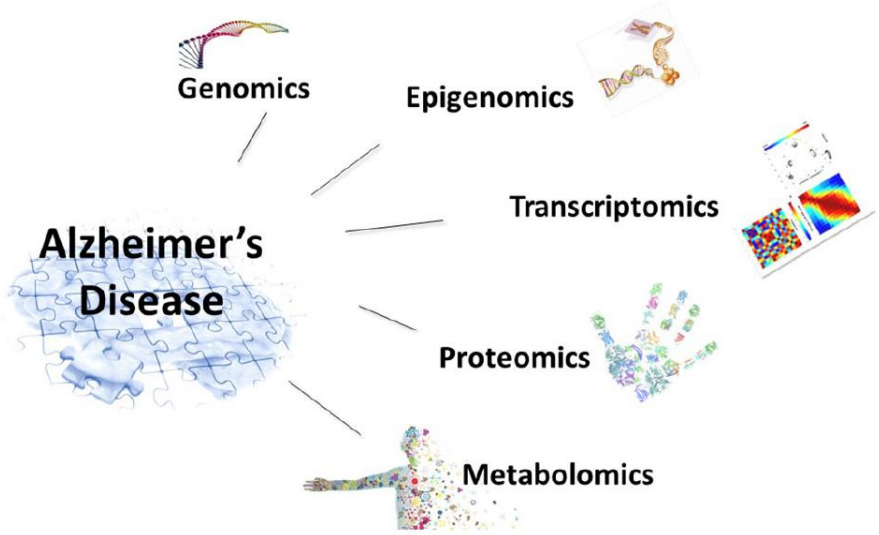

Figure 6. Multi-Omics approach in Alzheimer's disease (Sancesario & Bernardini, 2018).

Part II: Bioinformatics part

The reader is referred to the following files:

- AnalysisFC_HM450k.pdf
- QC_ncRNAs.pdf
- Analysis_ncRNAs.pdf

References

Anders, S., Pyl, P. T., & Huber, W. (2015). HTSeq—a Python framework to work with high-throughput sequencing data. *Bioinformatics, 31(2),* 166–169. https://doi.org/10.1093/bioinformatics/btu638

Babraham Bioinformatics (2018). FastQC. Consulted on 20/12/2018 from http://www.bioinformatics.babraham.ac.uk/projects/fastqc/

Baglietto-Vargas, D., Shi, J., Yaeger, D. M., Ager, R., & LaFerla, F. M. (2016). Diabetes and Alzheimer's disease crosstalk. *Neuroscience & Biobehavioral Reviews, 64*, 272–287. https://doi.org/10.1016/j.neubiorev.2016.03.005

Bolaños, J. P., Delgado-Esteban, M., Herrero-Mendez, A., Fernandez-Fernandez, S., & Almeida, A. (2008). Regulation of glycolysis and pentose–phosphate pathway by nitric oxide: Impact on neuronal survival. *Biochimica et Biophysica Acta (BBA) - Bioenergetics, 1777(7–8),* 789–793. https://doi.org/10.1016/j.bbabio.2008.04.011

Bolger, A. M., Lohse, M., & Usadel, B. (2014). Trimmomatic: a flexible trimmer for Illumina sequence data. *Bioinformatics, 30(15),* 2114–2120. https://doi.org/10.1093/bioinformatics/btu170

Braak, H., Alafuzoff, I., Arzberger, T., Kretzschmar, H., & Del Tredici, K. (2006). Staging of Alzheimer disease-associated neurofibrillary pathology using paraffin sections and immunocytochemistry. *Acta Neuropathologica*, 112(4), 389–404. https://doi.org/10.1007/s00401-006-0127-z

Cisternas, P., & Inestrosa, N. C. (2017). Brain glucose metabolism: Role of Wnt signaling in the metabolic impairment in Alzheimer's disease. *Neuroscience & Biobehavioral Reviews, 80*, 316–328. https://doi.org/10.1016/j.neubiorev.2017.06.004

Clement L. (2018, November), Statistical Genomics: Intro to RNA-seq - Arabidopsis.Rmd [Tutorial]. Ghent: Department of Applied mathematics, computer science and statistics, Ghent University. Consulted on 12/12/2018 from https://statomics.github.io/statisticalGenomicsCourse/pages/introToRNA-seqDE.html

Delhomme, N., Mähler, N., Schiffthaler, B., Sundell, D., Mannapperuma, C., Hvidsten, T.R. & Nathaniel R. Street, N.R. (2014). Guidelines for RNA-Seq data analysis [Tutorial]. Department of Biostatistics, Harvard School of Public Health, Boston, USA. Consulted on 20/12/2018 from https://www.epigenesys.eu/images/stories/protocols/pdf/20150303161357_p67.pdf

De Meyer, T. (2018, October 10th). Applied High-Throughput Analysis, Lecture 4: Infinium DNA methylation arrays, slide 60 [PowerPoint]. Ghent: Department of Data analysis and mathematical modelling, Ghent University.

De Meyer, T. (2018, October 24th). Applied High-Throughput Analysis, Lecture 5: SGS – Quality control, slide 29-35 [PowerPoint]. Ghent: Department of Data analysis and mathematical modelling, Ghent University.

De Meyer, T. (2018, November 7th). Applied High-Throughput Analysis, Lecture 6: SGS – Internal data-normalization, slide 23 [PowerPoint]. Ghent: Department of Data analysis and mathematical modelling, Ghent University.

De Meyer, T. (2018, November 7th). Applied High-Throughput Analysis, Lecture 6: SGS – DE testing, slide 52-55 [PowerPoint]. Ghent: Department of Data analysis and mathematical modelling, Ghent University.

Dobin, A., Davis, C. A., Schlesinger, F., Drenkow, J., Zaleski, C., Jha, S., … Gingeras, T. R. (2013). STAR: ultrafast universal RNA-seq aligner. *Bioinformatics, 29(1),* 15–21. https://doi.org/10.1093/bioinformatics/bts635

Du, P., Zhang, X., Huang, C.-C., Jafari, N., Kibbe, W. A., Hou, L., & Lin, S. M. (2010). Comparison of Beta-value and M-value methods for quantifying methylation levels by microarray analysis. *BMC Bioinformatics*, 11(1), 587. https://doi.org/10.1186/1471-2105-11-587

Durinck, S., Huber, W. and Smith, M. (2018, October 30th). The biomaRt users guide. R Package biomaRt 2.38.0. Consulted on 14/11/2018 from https://bioconductor.org/packages/release/bioc/vignettes/biomaRt/inst/doc/biomaRt.html

Gasparoni, G., Bultmann, S., Lutsik, P., Kraus, T. F. J., Sordon, S., Vlcek, J., … Walter, J. (2018). DNA methylation analysis on purified neurons and glia dissects age and Alzheimer's disease-specific changes in the human cortex. *Epigenetics & Chromatin*, 11(1). https://doi.org/10.1186/s13072-018-0211-3

González I. (2014, November 20th). Statistical analysis of RNA-Seq data [Tutorial]. France: Department of Bioinformatics/ Department of Biostatistics, INRA Toulouse/ IMT University Toulouse III. Consulted on 12/12/2018 from http://www.nathalievialaneix.eu/doc/pdf/tutorial-rnaseq.pdf

Guix, F. X., Raga, G., Bravo, R., et al. (2009). Amyloid-dependent triosephosphate isomerase nitrotyrosination induces glycation and tau fibrillation, *Brain, Volume 132*, 1335–1345, https://doi.org/10.1093/brain/awp023

Guo, J., Cheng, J., North, B. J., & Wei, W. (2017). Functional analyses of major cancer-related signaling pathways in Alzheimer's disease etiology. *Biochimica et Biophysica Acta (BBA) - Reviews on Cancer, 1868(2),* 341–358. https://doi.org/10.1016/j.bbcan.2017.07.001

Hansen, K. D., Brenner, S. E., & Dudoit, S. (2010). Biases in Illumina transcriptome sequencing caused by random hexamer priming*. Nucleic Acids Research, 38(12),* e131. https://doi.org/10.1093/nar/gkq224

Hokama, M., Oka, S., Leon, J., Ninomiya, T., Honda, H., Sasaki, K., … Nakabeppu, Y. (2014). Altered Expression of Diabetes-Related Genes in Alzheimer's Disease Brains: The Hisayama Study. *Cerebral Cortex*, 24(9), 2476–2488. https://doi.org/10.1093/cercor/bht101

Huang, W.-J., Zhang, X., & Chen, W.-W. (2016). Role of oxidative stress in Alzheimer's disease. *Biomedical Reports, 4(5),* 519–522. https://doi.org/10.3892/br.2016.630

Illumina (2018). Illumina Adapter Sequences. Consulted on 20/12/2018 from http://emea.support.illumina.com/content/dam/illumina-support/documents/documentation/chemistry_documentation/experiment-design/illumina-adapter-sequences-1000000002694-09.pdf

Ip, C. (1998). Lessons from basic research in selenium and cancer prevention. *The Journal of Nutrition. 128 (11),* 1845–54. https://doi.org/10.1093/jn/128.11.1845

Lau, P., Bossers, K., Janky, R., Salta, E., Frigerio, C. S., Barbash, S., … De Strooper, B. (2013). Alteration of the microRNA network during the progression of Alzheimer's disease: Profiling of microRNAs in Alzheimer's disease. *EMBO Molecular Medicine*, *5(10),* 1613–1634. https://doi.org/10.1002/emmm.201201974

Law, CW, Chen, Y, Shi, W, and Smyth, GK (2014). Voom: precision weights unlock linear model analysis tools for RNA-seq read counts*. Genome Biology 15*, R29.

Love MI, Huber W, Anders S (2014). Moderated estimation of fold change and dispersion for RNA-seq data with DESeq2. *Genome Biology, 15*, 550. doi: 10.1186/s13059-014-0550-8.

Lunnon, K., & Mill, J. (2013). Epigenetic studies in Alzheimer's disease: Current findings, caveats, and considerations for future studies. *American Journal of Medical Genetics Part B: Neuropsychiatric Genetics, 162(8),* 789–799. https://doi.org/10.1002/ajmg.b.32201

Manczak, M., & Reddy, P. H. (2013). RNA silencing of genes involved in Alzheimer's disease enhances mitochondrial function and synaptic activity. *Biochimica et Biophysica Acta (BBA) - Molecular Basis of Disease, 1832(12),* 2368–2378. https://doi.org/10.1016/j.bbadis.2013.09.008

McCarthy DJ, Chen Y and Smyth GK (2012). Differential expression analysis of multifactor RNA-Seq experiments with respect to biological variation. *Nucleic Acids Research 40,* 4288-4297

Nativio, R., Donahue, G., Berson, A., Lan, Y., Amlie-Wolf, A., Tuzer, F., … Berger, S. L. (2018). Dysregulation of the epigenetic landscape of normal aging in Alzheimer's disease. *Nature Neuroscience, 21(4),* 497–505. https://doi.org/10.1038/s41593-018-0101-9

NCBI Gene (2018). AP1B1, consulted on 17/11/2018 from https://www.ncbi.nlm.nih.gov/gene/162

NCBI Gene (2018). CFAP70, consulted on 17/11/2018 from https://www.ncbi.nlm.nih.gov/gene/118491

NCBI Gene (2018). CGGBP1, consulted on 17/11/2018 from https://www.ncbi.nlm.nih.gov/gene/8545

NCBI Gene (2018). DEFB123, consulted on 17/11/2018 from https://www.ncbi.nlm.nih.gov/gene/245936

NCBI Gene (2018). GNS, consulted on 17/11/2018 from https://www.ncbi.nlm.nih.gov/gene/2799/

NCBI Gene (2018). HSP90AA1, consulted on 17/11/2018 from https://www.ncbi.nlm.nih.gov/gene/3320

NCBI Gene (2018). JRKL-AS1, consulted on 17/11/2018 from https://www.ncbi.nlm.nih.gov/gene/?term=JRKL-AS1

NCBI Gene (2018). LOC285889, consulted on 17/11/2018 from https://www.ncbi.nlm.nih.gov/gene/?term=LOC285889

NCBI Gene (2018). LOC646903, consulted on 17/11/2018 from https://www.ncbi.nlm.nih.gov/gene/?term=LOC646903

NCBI Gene (2018). MBP, consulted on 17/11/2018 from https://www.ncbi.nlm.nih.gov/gene/4155

NCBI Gene (2018). MIR4225, consulted on 17/11/2018 from https://www.ncbi.nlm.nih.gov/gene/?term=MIR4255

NCBI Gene (2018). MND1, consulted on 17/11/2018 from https://www.ncbi.nlm.nih.gov/gene/84057

NCBI Gene (2018). NAGLU, consulted on 17/11/2018 from https://www.ncbi.nlm.nih.gov/gene/4669

NCBI Gene (2018). NDN, consulted on 17/11/2018 from https://www.ncbi.nlm.nih.gov/gene/4692

NCBI Gene (2018). NUB1, consulted on 17/11/2018 from https://www.ncbi.nlm.nih.gov/gene/51667

NCBI Gene (2018). NWD1, consulted on 17/11/2018 from https://www.ncbi.nlm.nih.gov/gene/284434

NCBI Gene (2018). PPP3CC, consulted on 17/11/2018 from https://www.ncbi.nlm.nih.gov/gene/5533

NCBI Gene (2018). RPSAP9, consulted on 17/11/2018 from https://www.ncbi.nlm.nih.gov/gene/653162

NCBI Gene (2018). SLC4A8, consulted on 17/11/2018 from https://www.ncbi.nlm.nih.gov/gene/9498

NCBI Gene (2018). SRF, consulted on 17/11/2018 from https://www.ncbi.nlm.nih.gov/gene/6722

NCBI Gene (2018). TFCP2, consulted on 17/11/2018 from https://www.ncbi.nlm.nih.gov/gene?cmd=retrieve&dopt=default&rn=1&list_uids=7024

NCBI Gene (2018). THEGL, consulted on 17/11/2018 from https://www.ncbi.nlm.nih.gov/gene/100506564

NCBI Gene (2018). TIGD1, consulted on 17/11/2018 from https://www.ncbi.nlm.nih.gov/gene/200765

NCBI Gene (2018). WNT1, consulted on 17/11/2018 from https://www.ncbi.nlm.nih.gov/gene/7472

NCBI Gene (2018). XYLT2, consulted on 17/11/2018 from https://www.ncbi.nlm.nih.gov/gene/64132

NCBI Gene (2018). ZC3H12B, consulted on 17/11/2018 from https://www.ncbi.nlm.nih.gov/gene/340554

NCBI MedGen (2018). Mucopolysaccharidosis MPS-III-B, consulted on 17/11/2018 from https://www.ncbi.nlm.nih.gov/medgen/?term=Sanfilippo+syndrome+B

Picón-Pagès, P., Garcia-Buendia, J., Muñoz, F.J. (2018). Functions and dysfunctions of nitric oxide in brain. *BBA - Molecular Basis of Disease, In press,* https://doi.org/10.1016/j.bbadis.2018.11.007

Pidsley, Ruth, Wong Y, C C, Volta, Manuela, Lunnon, Katie, Mill, Jonathan, Schalkwyk, C L (2013). A data-driven approach to preprocessing Illumina 450K methylation array data. *BMC Genomics, 14,* 293. doi: 10.1186/1471-2164-14-293.

Sancesario, G. M., & Bernardini, S. (2018). Alzheimer's disease in the omics era. *Clinical Biochemistry, 59,* 9–16. https://doi.org/10.1016/j.clinbiochem.2018.06.011

Schalkwyk L.C. et al. (2018). Package wateRmelon from Bioconductor: Dasen (30/11/2018), 13-14. https://www.rdocumentation.org/packages/wateRmelon/versions/1.16.0/topics/dasen-methods

Sperling, R. A., Aisen, P. S., Beckett, L. A., Bennett, D. A., Craft, S., Fagan, A. M., … Phelps, C. H. (2011). Toward defining the preclinical stages of Alzheimer's disease: Recommendations from the National Institute on Aging-Alzheimer's Association workgroups on diagnostic guidelines for Alzheimer's disease. *Alzheimer's & Dementia, 7(3),* 280–292. https://doi.org/10.1016/j.jalz.2011.03.003

Ritchie ME, Phipson B, Wu D, Hu Y, Law CW, Shi W, Smyth GK (2015). Limma powers differential expression analyses for RNA-sequencing and microarray studies. *Nucleic Acids Research, 43(7),* e47.

Robinson MD, McCarthy DJ and Smyth GK (2010). edgeR: a Bioconductor package for differential expression analysis of digital gene expression data. *Bioinformatics 26*, 139-140

Roy, A., & Bhattacharyya, M. (2016). Identifying microRNAs related to Alzheimer's disease from differential methylation signatures. *Gene Reports, 4,* 104–111. https://doi.org/10.1016/j.genrep.2016.04.006

Triche, Jr. T (2014). FDb.InfiniumMethylation.hg19: Annotation package for Illumina Infinium DNA methylation probes. R package version 2.2.0. Consulted on 14/11/2018 from https://bioconductor.org/packages/release/data/annotation/manuals/FDb.InfiniumMethylation.hg19/man/FDb.InfiniumMethylation.hg19.pdf

UniprotKB (2018). A0FGR8, consulted on 17/11/2018 from https://www.uniprot.org/uniprot/A0FGR8

UniprotKB (2018). A6NI61, consulted on 17/11/2018 from https://www.uniprot.org/uniprot/A6NI61

UniprotKB (2018). G8NES3, consulted on 17/11/2018 from https://www.uniprot.org/uniprot/Q8NES3

UniprotKB (2018). O43261, consulted on 17/11/2018 from https://www.uniprot.org/uniprot/O43261

UniprotKB (2018). P02686, consulted on 17/11/2018 from https://www.uniprot.org/uniprot/P02686

UniprotKB (2018). P09455, consulted on 17/11/2018 from https://www.uniprot.org/uniprot/P09455

UniprotKB (2018). P0DJG4, consulted on 17/11/2018 from https://www.uniprot.org/uniprot/P0DJG4

UniprotKB (2018). P1183, consulted on 17/11/2018 from https://www.uniprot.org/uniprot/P1183

UniProtKB (2018). P15586, consulted on 17/11/2018 from https://www.uniprot.org/uniprot/P15586

UniprotKB (2018). P15848, consulted on 17/11/2018 from https://www.uniprot.org/uniprot/P15848

UniprotKB (2018). P43304, consulted on 17/11/2018 from https://www.uniprot.org/uniprot/P43304

UniprotKB (2018). P48454, consulted on 17/11/2018 from https://www.uniprot.org/uniprot/P48454

UniprotKB (2018). P54802, consulted on 17/11/2018 from https://www.uniprot.org/uniprot/P54802

UniprotKB (2018). Q10567, consulted on 17/11/2018 from https://www.uniprot.org/uniprot/Q10567

UniprotKB (2018). Q13105, consulted on 17/11/2018 from https://www.uniprot.org/uniprot/Q13105

UniprotKB (2018). Q6H8Q1, consulted on 17/11/2018 from https://www.uniprot.org/uniprot/Q6H8Q1

UniprotKB (2018). Q6S8J3, consulted on 17/11/2018 from https://www.uniprot.org/uniprot/Q6S8J3

UniprotKB (2018). Q7Z3K6, consulted on 17/11/2018 from https://www.uniprot.org/uniprot/Q7Z3K6

UniprotKB (2018). Q86XL3, consulted on 17/11/2018 from https://www.uniprot.org/uniprot/Q86XL3

UniprotKB (2018). Q8NBF2, consulted on 17/11/2018 from https://www.uniprot.org/uniprot/Q8NBF2

UniprotKB (2018). Q92802, consulted on 17/11/2018 from https://www.uniprot.org/uniprot/Q92802

UniprotKB (2018). Q96F07, consulted on 17/11/2018 from https://www.uniprot.org/uniprot/Q96F07

UniprotKB (2018). Q96MW7, consulted on 17/11/2018 from https://www.uniprot.org/uniprot/Q96MW7

UniprotKB (2018). Q96NM4, consulted on 17/11/2018 from https://www.uniprot.org/uniprot/Q96NM4

UniprotKB (2018). Q96SA4, consulted on 17/11/2018 from https://www.uniprot.org/uniprot/Q96SA4

UniprotKB (2018). Q99963, consulted on 17/11/2018 from https://www.uniprot.org/uniprot/Q99963

UniprotKB (2018). Q9BRQ6, consulted on 17/11/2018 from https://www.uniprot.org/uniprot/Q9BRQ6

UniprotKB (2018). Q9BRV8, consulted on 17/11/2018 from https://www.uniprot.org/uniprot/Q9BRV8

UniprotKB (2018). Q9BTF0, consulted on 17/11/2018 from https://www.uniprot.org/uniprot/Q9BTF0

UniprotKB (2018). Q9H1B5, consulted on 17/11/2018 from https://www.uniprot.org/uniprot/Q9H1B5

UniprotKB (2018). Q9NVP4, consulted on 17/11/2018 from https://www.uniprot.org/uniprot/Q9NVP4

UniprotKB (2018). Q9UFH2, consulted on 17/11/2018 from https://www.uniprot.org/uniprot/Q9UFH2

UniprotKB (2018). Q9UFW8, consulted on 17/11/2018 from https://www.uniprot.org/uniprot/Q9UFW8

UniprotKB (2018). Q9ULW0, consulted on 17/11/2018 from https://www.uniprot.org/uniprot/Q9ULW0

UniprotKB (2018). Q9Y2G7, consulted on 17/11/2018 from https://www.uniprot.org/uniprot/Q9Y2G7

UniprotKB (2018). Q9Y2M2, consulted on 17/11/2018 from https://www.uniprot.org/uniprot/Q9Y2M2

UniprotKB (2018). Q9Y4A0, consulted on 17/11/2018 from https://www.uniprot.org/uniprot/Q9Y4A0
UniprotKB (2018). Q9Y5A7, consulted on 17/11/2018 from https://www.uniprot.org/uniprot/Q9Y5A7

UniprotKB (2018). Q9Y6I4, consulted on 17/11/2018 from https://www.uniprot.org/uniprot/Q9Y6I4

Wang, J., Vasaikar, S., Shi, Z., Greer, M., & Zhang, B. (2017). WebGestalt 2017: a more comprehensive, powerful, flexible and interactive gene set enrichment analysis toolkit. *Nucleic Acids Research, Volume 45*, W130–W137, https://doi.org/10.1093/nar/gkx356

Wang, Z.-T., Tan, C.-C., Tan, L., & Yu, J.-T. (2019). Systems biology and gene networks in Alzheimer's disease. *Neuroscience & Biobehavioral Reviews, 96*, 31–44. https://doi.org/10.1016/j.neubiorev.2018.11.007

Yin, F., Sancheti, H., Patil, I., & Cadenas, E. (2016). Energy metabolism and inflammation in brain aging and Alzheimer's disease. *Free Radical Biology and Medicine, 100*, 108–122. https://doi.org/10.1016/j.freeradbiomed.2016.04.200

Zendjabil, M. (2018). Circulating microRNAs as novel biomarkers of Alzheimer's disease. *Clinica Chimica Acta, 484*, 99–104. https://doi.org/10.1016/j.cca.2018.05.039

Supplementary Tables

Table 1. Degree of braak stages and the corresponding affected regions (Braak et al., 2006).

Braak stage	Affected region in the brain
I	Transentorhinal region
II	Extension to entorhinal region
III	Spreading toward neocortex of the fusiform and lingual gyri
IV	Expansion into neocortical association areas
V	Extension to frontal, superolateral, and occipital directions. Eventually reaching the peristriate region
VI	Secondary and primary neocortical areas and the occipital lobe are reached, further spreading into the striate area

Table 2. Results hypermethylated CpGs (p<0.05).

Probe	Distance	Gene	M difference	logFC	AveExpr	Adjusted P
cg05206762	178	ABLIM2	0,02419	0,193488	-1,56218	0,015249
cg17772535	9	GNS	0,077117	0,186876	-2,05567	0,016694
cg01145559	255	HSP90AA1	0,044857	0,166191	-2,20218	0,025018
cg19381780	142	ZFP30	0,065128	0,174174	-2,5352	0,025056
cg02760007	456	SRF	0,082096	0,174312	-1,57692	0,026149
cg20938157	106	CYFIP2	0,041022	0,17978	-2,04695	0,026149
cg16314291	73	SERINC2	0,01287	0,232784	-2,15909	0,029816
cg15653194	4	LFNG	0,083736	0,16376	-2,31852	0,031815
cg05516986	154	ESYT2	0,121081	0,178067	-2,21873	0,032607
cg14230859	561	GPD2	0,016663	-0,31988	1,266497	0,039971
cg14051306	288	MIER3	0,06458	0,170583	-2,66072	0,04718

Table 3. Results hypomethylated CpGs (p<0.05).

Probe	Distance	Gene	M difference	logFC	AveExpr	Adjusted P
cg19165344	782	AP1B1	-0,04326	-0,24481	1,142788	0,004216
cg10550471	1267	LOC285889	-0,12698	-0,42591	1,942193	0,005585
cg27105914	65	DNAH17	-0,07712	-0,35739	1,470406	0,007872
cg19110428	1990	TPX2	-0,08078	-0,48903	1,31289	0,008442
cg02193513	1761	THEGL	-0,10005	-0,39208	1,318334	0,00855
cg09380357	360	NUB1	-0,11249	-0,38256	1,164521	0,00855
cg23392359	1263	ARSB	-0,18363	-0,33843	2,066664	0,009294
cg18346402	2450	TIGD1	-0,01581	-0,43635	0,350459	0,009294
cg16830479	839	ZC3H12B	-0,14121	-0,36099	0,844498	0,009294
cg20623645	557	NAGLU	-0,00184	-0,34075	0,532426	0,009294
cg03338185	2193	ZBTB17	-0,13349	-0,45267	0,835379	0,013275
cg08961047	1235	RPS10-NUDT3	-0,18525	-0,40127	2,984867	0,013275
cg24400553	1110	ABHD17A	-0,11527	-0,25047	1,509891	0,015615

cg24163448	69	RPSAP9	-0,10486	-0,41501	1,02759	0,015615
cg27021666	1232	HSPA1B	-0,12154	-0,3601	1,660872	0,016694
cg06074994	1445	WNT2	-0,13143	-0,20708	-3,2347	0,017815
cg05207611	1531	ANKLE2	-0,11136	-0,26778	1,720635	0,017815
cg21276022	167	MYMK	-0,11193	-0,25396	2,09996	0,017815
cg12774482	58	DLEU1	-0,11819	-0,20549	-3,068	0,019922
cg15495901	800	NWD1	-0,05644	-0,2431	0,153428	0,022799
cg13758646	1766	GABBR2	-0,06667	-0,15359	-2,98909	0,025018
cg01052854	3	SIKE1	-0,03654	-0,16122	-3,11736	0,026149
cg05616792	763	MBP	-0,1009	-0,1922	-3,02494	0,026417
cg05052501	2181	C8orf34	-0,14845	-0,24634	1,106111	0,02664
cg00971891	378	CGGBP1	-0,0663	-0,15766	-2,68023	0,026828
cg19788417	771	DEFB123	-0,05873	-0,2427	0,508635	0,027211
cg09456065	2319	MNS1	-0,09304	-0,29491	0,701171	0,029585
cg23969515	296	XYLT2	-0,09381	-0,16667	-3,01627	0,030325
cg14129397	1556	NPTX1	-0,03506	-0,1842	-3,15878	0,031476
cg19544510	20	SSUH2	-0,06403	-0,36707	1,485781	0,031577
cg13254588	100	THUMPD2	-0,08777	-0,20352	-2,93068	0,031577
cg03341991	79	N4BP2L2	-0,09889	-0,19106	-3,27356	0,032882
cg08941759	23	CHCHD6	-0,07583	-0,15448	-3,40591	0,03567
cg15708153	63	ZNF542P	-0,11401	-0,1794	-3,30837	0,035839
cg24415793	159	SLC4A8	-0,05273	-0,24033	-1,86345	0,036962
cg14261700	24	NHLRC2	-0,08456	-0,16752	-3,16876	0,040013
cg12653788	1611	CCDC185	-0,03459	-0,21797	1,245519	0,040013
cg02731042	207	L3MBTL4	-0,12914	-0,18393	-3,02392	0,042075
cg11116878	630	TRDMT1	-0,06829	-0,14629	-3,50655	0,04334
cg02881331	7	EFCAB5	-0,0016	0,177781	-1,52171	0,045499
cg13582500	1491	ZDHHC5	-0,08079	-0,2381	0,935054	0,04553
cg03227184	91	TMEM155	-0,00323	-0,17746	-2,3898	0,04553
cg10701168	1153	SLC13A2	-0,07034	-0,27329	1,513355	0,04553
cg14334147	1349	SNX12	-0,11266	-0,45805	0,854556	0,04553
cg20554926	55	NUDCD2	-0,04322	-0,1652	-3,11373	0,04553
cg07925549	729	KRT75	-0,04343	-0,18505	2,175636	0,04553
cg11356706	581	SRXN1	-0,11072	-0,20963	-2,64518	0,046338
cg18884940	2152	SNORD93	-0,04288	-0,13022	-3,45608	0,04718
cg17398066	73	FAM172A	-0,04461	-0,15151	-3,22026	0,04718
cg00787919	392	MND1	-0,16264	-0,22838	-3,38403	0,04718
cg14792983	79	DZANK1	-0,05231	-0,16728	-2,29477	0,04718
cg12642414	25	USP3	-0,04104	-0,17782	-3,27366	0,047669
cg22830663	172	POTEE	-0,07759	-0,24574	1,297099	0,048294
cg17533458	331	MIR2277	-0,07037	-0,17496	-2,94769	0,048294
cg02910208	2	VSTM2A	-0,10855	-0,15829	-3,13796	0,048294
cg16446585	1879	MELTF	-0,06466	-0,22487	2,918064	0,048294

Table 4. Basic characteristics of sample SRR1103948 (ncRNA dataset).

Measure	Value
Filename	*SRR1103948.fastq*
File type	*Conventional base calls*
Encoding	*Sanger / Illumina 1.9*
Total Sequences	*16194562*
Filtered Sequences	*0*
Sequence length	*36*
%GC	*50*

Table 5. Selection of involved KEGG pathways for methylation dataset GSE66351.

ID KEGG	Pathway	Adjusted P-Value
hsa00010	Glycolysis / Gluconeogenesis	1
hsa00020	Citrate cycle (TCA cycle)	1
hsa00030	Pentose phosphate pathway	1
hsa00040	Pentose and glucuronate interconversions	1
hsa00051	Fructose and mannose metabolism	1
hsa00052	Galactose metabolism	1
hsa01100	Metabolic pathways	1
hsa01200	Carbon metabolism	1
hsa03008	Ribosome biogenesis in eukaryotes	1
hsa03010	Ribosome	1
hsa03013	RNA transport	1
hsa04010	MAPK signaling pathway	1
hsa04012	ErbB signaling pathway	1
hsa04014	Ras signaling pathway	1
hsa04015	Rap1 signaling pathway	1
hsa04020	Calcium signaling pathway	1
hsa04022	cGMP-PKG signaling pathway	1
hsa04024	cAMP signaling pathway	1
hsa04060	Cytokine-cytokine receptor interaction	1
hsa04066	HIF-1 signaling pathway	1
hsa04080	Neuroactive ligand-receptor interaction	1
hsa04110	Cell cycle	1
hsa04210	Apoptosis	1
hsa04668	TNF signaling pathway	1
hsa04750	Inflammatory mediator regulation of TRP channels	1
hsa04810	Regulation of actin cytoskeleton	1
hsa04910	Insulin signaling pathway	1
hsa04931	Insulin resistance	1
hsa04940	Type I diabetes mellitus	1
hsa05010	Alzheimer disease	1
hsa05012	Parkinson disease	1

Table 6. Top 20 of GSA for ncRNA dataset GSE48552.

GO Accession	Pathway	Adjusted P-Value
GO:1903231	mRNA binding involved in posttranscriptional gene silencing	2,46E-21
GO:0035195	gene silencing by miRNA	7,49E-18
GO:0035194	posttranscriptional gene silencing by RNA	9,93E-18
GO:0016441	posttranscriptional gene silencing	1,03E-17
GO:0031047	gene silencing by RNA	2,8E-17
GO:0003729	mRNA binding	6,15E-17
GO:0017148	negative regulation of translation	2,39E-16
GO:0034249	negative regulation of cellular amide metabolic process	3,91E-16
GO:0016458	gene silencing	6,88E-16
GO:0040029	regulation of gene expression, epigenetic	2,73E-15
GO:0006417	regulation of translation	3,71E-14
GO:0034248	regulation of cellular amide metabolic process	9,26E-14
GO:0010608	posttranscriptional regulation of gene expression	4,85E-13
GO:0006412	translation	5,09E-12
GO:0005615	extracellular space	6,17E-12
GO:0043043	peptide biosynthetic process	7,52E-12
GO:0044421	extracellular region part	1,9E-11
GO:0043604	amide biosynthetic process	2,27E-11
GO:0006518	peptide metabolic process	6,06E-11
GO:0043603	cellular amide metabolic process	4,05E-10

Table 7. Selection of involved KEGG pathways for ncRNA dataset GSE48552.

ID KEGG	Pathway	Adjusted P-Value
hsa05206	MicroRNAs in cancer	1,73E-16
hsa00010	Glycolysis / Gluconeogenesis	1
hsa00020	Citrate cycle (TCA cycle)	1
hsa00030	Pentose phosphate pathway	1
hsa00051	Fructose and mannose metabolism	1
hsa00052	Galactose metabolism	1
hsa00190	Oxidative phosphorylation	1
hsa01100	Metabolic pathways	1
hsa01200	Carbon metabolism	1
hsa03008	Ribosome biogenesis in eukaryotes	1
hsa03013	RNA transport	1
hsa03018	RNA degradation	1
hsa04010	MAPK signaling pathway	1
hsa04014	Ras signaling pathway	1
hsa04015	Rap1 signaling pathway	1
hsa04024	cAMP signaling pathway	1
hsa04060	Cytokine-cytokine receptor interaction	1
hsa04066	HIF-1 signaling pathway	1
hsa04068	FoxO signaling pathway	1
hsa04072	Phospholipase D signaling pathway	1
hsa04080	Neuroactive ligand-receptor interaction	1
hsa04110	Cell cycle	1

hsa04114	Oocyte meiosis	1
hsa04144	Endocytosis	1
hsa04150	mTOR signaling pathway	1
hsa04151	PI3K-Akt signaling pathway	1
hsa04152	AMPK signaling pathway	1
hsa04210	Apoptosis	1
hsa04310	Wnt signaling pathway	1
hsa04510	Focal adhesion	1
hsa04514	Cell adhesion molecules (CAMs)	1
hsa04668	TNF signaling pathway	1
hsa04810	Regulation of actin cytoskeleton	1
hsa04910	Insulin signaling pathway	1
hsa05010	Alzheimer disease	1
hsa05012	Parkinson disease	1

Table 8. Functions of annotated genes within distance of 2500 bp from the probe.

Gene	Name	(one of the) Functions	Source
ABLIM2	Actin-binding LIM protein 2	Actin filament binding and organization	UniprotKB Q6H8Q1 (2018).
ANKLE2	Ankyrin repeat and LEM domain-containing 2	Regulation of catalytic activity, CNS development, mitotic nuclear envelope reassembly, negative regulation of apoptotic process and phosphorylation, positive regulation of protein dephosphorylation, cell division	UniprotKB Q86XL3 (2018).
AP1B1	AP-1 complex subunit beta-1	Recruitment of clathrin protein (role in the formation of coated vesicles)	NCBI Gene AP1B1 (2018). UniprotKB Q10567 (2018).
ARSB	Arylsulfatase B	Autophagy, CNS development, degradation of sulfate groups from chondroitin-4-sulfate	UniprotKB P15848 (2018).
CFAP70	Cilia and flagella associated protein 70	Cell mobility	NCBI Gene CFAP70 (2018).
CGGBP1	CGG triplet repeat binding protein 1	Negative regulation of transcription by RNA polymerase II, DNA damage repair, telomere protection	UniprotKB Q9UFW8 (2018). NCBI Gene CGGBP1 (2018).
CHCHD6	Coiled-coil-helix-coiled-coil-helix domain containing 6	Cellular response to DNA damage stimulus	UniprotKB Q9BRQ6 (2018).
CYFIP2	Cytoplasmic FMR1-interacting protein 2	Apoptosis	UniprotKB Q96F07 (2018).
DEFB123	Defensin beta 123	Host immunologic response to invading microorganisms	NCBI Gene DEFB123 (2018).
DLEU1	Deleted in lymphocytic leukemia 1	Tumor repressor	UniprotKB O43261 (2018).
DNAH17	Dynein axonemal heavy chain 17	Cell mobility	UniprotKB Q9UFH2 (2018).
DZANK1	Double zinc ribbon and ankyrin repeat domains 1	Metal ion binding	UniprotKB Q9NVP4 (2018).
ESYT2	Extended synaptotagmin 2	Endocytosis, lipid transport	UniprotKB A0FGR8 (2018).
GNS	Glucosamine (N-acetyl)-6-sulfatase	Hydrolysis of N-acetyl-D-glucosamine 6-sulfate units of heparin	NCBI Gene GNS (2018).
GPD2	Glycerol-3-phosphate dehydrogenase 2	Gluconeogenesis, constitution of the glycerol phosphate shuttle	UniprotKB P43304 (2018).
HSP90AA1	Heat shock protein 90 alpha family class A member 1	Folding of specific target proteins by use of an ATPase activity	NCBI Gene HSP90AA1 (2018).
JRKL-AS1	JRKL antisense RNA 1	CNS development	UniprotKB Q9Y4A0 (2018). NCBI Gene JRKL-AS1 (2018).
LFNG	O-fucosylpeptide 3-beta-N-acetylglucosaminyltransferase	Regulation of somitogenesis	UniprotKB G8NES3 (2018).
LOC285889	Uncharacterized ncRNA	Unknown	NCBI Gene LOC285889 (2018).
LOC646903	Uncharacterized ncRNA	Unknown	NCBI Gene LOC646903 (2018).

N4BP2L2	NEDD4 binding protein 2 like 2	Negative regulation of hematopoietic stem cell differentiation, negative regulation of transcription by RNA polymerase II, positive regulation of hematopoietic stem cell proliferation	UniprotKB Q92802 (2018).
NAGLU	N-acetyl-alpha-glucosaminidase	Degradation of heparan sulfate, development of the nervous system	UniprotKB P54802 (2018). NCBI Gene NAGLU (2018).
NDN	Necdin	Prader-Willi syndrome, suppression postmitotic neurons growth	NCBI Gene NDN (2018).
NHLRC2	NHL repeat containing 2	Cell redox homeostasis, platelet degranulation	UniprotKB Q8NBF2 (2018).
NUB1	Negative regulator of ubiquitin like proteins 1	Negative regulator of NEDD8 (is accumulated in Lewy bodies in Parkinson's disease and dementia), production of tumor necrosis factors	NCBI Gene NUB1 (2018). UniprotKB Q9Y5A7 (2018).
NWD1	NACHT and WD repeat domain containing 1	Increased expression observed in some prostate cancer cell lines, regulation of androgen receptor activity	NCBI Gene NWD1 (2018).
MBP	Myelin basic protein	Myelin sheath of oligodendrocytes and Schwann cells in nervous system, transcripts are present in the bone marrow and the immune system, involved in signaling pathways in T-cells and neural cells	UniprotKB P02686 (2018). NCBI Gene MBP (2018).
MIER3	Mesoderm induction early response family member 3	Transcriptional repressor, negative regulation of transcription by RNA polymerase II, histone deacetylation	UniprotKB Q7Z3K6 (2018).
MIR4255	microRNA 4255	Influences post-transcriptional regulation of gene expression by affecting stability and translation of mRNAs	NCBI Gene MIR4225 (2018).
MND1	Meiotic nuclear divisions 1	Meiotic recombination	NCBI Gene MND1 (2018).
MYMK	Myomaker	Myoblast fusion factor	UniprotKB A6NI61 (2018).
POTEE	POTE ankyrin domain family member E	Retina homeostasis, brain development	UniprotKB Q6S8J3 (2018).
PPP3CC	Protein phosphatase 3 catalytic subunit gamma	Brain development, downstream regulation of dopaminergic signal transduction	UniprotKB P48454 (2018). NCBI Gene PPP3CC (2018).
RBP1	Retinol binding protein 1	Retinol transport, lipid homeostasis, retinoid and vitamin A metabolic process	UniprotKB P09455 (2018).
RPSAP9	Ribosomal protein SA pseudogene 9	Not clear	NCBI Gene RPSAP9 (2018).
SERINC2	Serine incorporator 2	Phosphatidylserine and sphingolipid metabolic process	UniprotKB Q96SA4 (2018).
SH3GL3	SH3 domain containing GRB2 like 3, endophilin A3	Negative regulation of clathrin-dependent endocytosis, CNS development , positive regulation of neuron differentiation , signal transduction	UniprotKB Q99963 (2018).
SIKE1	Suppressor of IKBKE 1	Physiological suppressor of IKK-epsilon and TBK1→ inhibition of virus- and TLR3-triggered IRF3	UniprotKB Q9BRV8 (2018).
SLC4A8	Solute carrier family 4 member 8	Transport of sodium and bicarbonate ions across the cell membrane, pH regulation in neurons	NCBI Gene SLC4A8 (2018).
SSUH2	Protein SSUH2 homolog	Odontogenesis (=progression of a tooth or teeth)	UniprotKB Q9Y2M2 (2018).
SRF	Serum response factor	Long-term memory, negative regulation of amyloid-beta clearance, neuron development, neuron migration, neuron projection development,	UniprotKB P1183 (2018). NCBI Gene SRF (2018).

		positive regulation of transcription by RNA polymerase II and pri-miRNA transcription, cell proliferation and differentiation, cell cycle regulation, apoptosis, cell growth and differentiation, downstream target of MAPK pathway	
TFCP2	Transcription factor CP2	Activation of alpha-globin gene which polymorphisms play a role in the pathogenesis of Alzheimer's disease, regulation of erythroid gene expression, transcriptional switch of globin gene promoters, activation cellular and viral gene promoters, interaction with inflammatory response factors	NCBI Gene TFCP2 (2018).
THEGL	Testicular haploid expressed gene protein-like	Not clear	UniprotKB P0DJG4 (2018). NCBI Gene THEGL (2018).
THUMPD2	THUMP domain containing 2	tRNA methylation	UniprotKB Q9BTF0 (2018).
TIGD1	Tigger transposable element-derived 1	DNA binding, exact function unknown, proteins are related to DNA transposons found in fungi and nematode	UniprotKB Q96MW7 (2018). NCBI Gene TIGD1 (2018).
TOX2	TOX high mobility group box family member 2	Positive regulation of transcription by RNA polymerase II, DNA binding	UniprotKB Q96NM4 (2018).
TPX2	Targeting protein for Xklp2	Apoptosis, cell proliferation	UniprotKB Q9ULW0 (2018).
USP3	Ubiquitin specific peptidase 3	DNA repair, negative regulation of transcription by RNA polymerase II, histone deubiquitination, protein deubiquitination, regulation of protein stability, ubiquitin-dependent protein catabolic process	UniprotKB Q9Y6I4 (2018).
WNT2	Wnt family member 2	Oncogenesis, regulation of cell fate and patterning during embryogenesis	NCBI Gene WNT1 (2018).
XYLT2	Xylosyltransferase 2	Transfer of D-xylose from UDP-D-xylose to specific serine residues of the core protein, catalysis of the first step in the biosynthesis of chondroitin sulfate, heparan sulfate and dermatan sulfate proteoglycans which is increased in scleroderma patients	UniprotKB Q9H1B5 (2018). NCBI Gene XYLT2 (2018).
ZBTB17	Zinc finger and BTB domain-containing protein 17	Positive regulation of transcription by RNA polymerase II, DNA binding	UniprotKB Q13105 (2018).
ZC3H12B	Zinc finger CCCH-type containing 12B	Proinflammatory activation of macrophages	NCBI Gene ZC3H12B (2018).
ZFP30	Zinc finger protein 30	Transcription regulation	UniprotKB Q9Y2G7 (2018).

Supplementary Figures

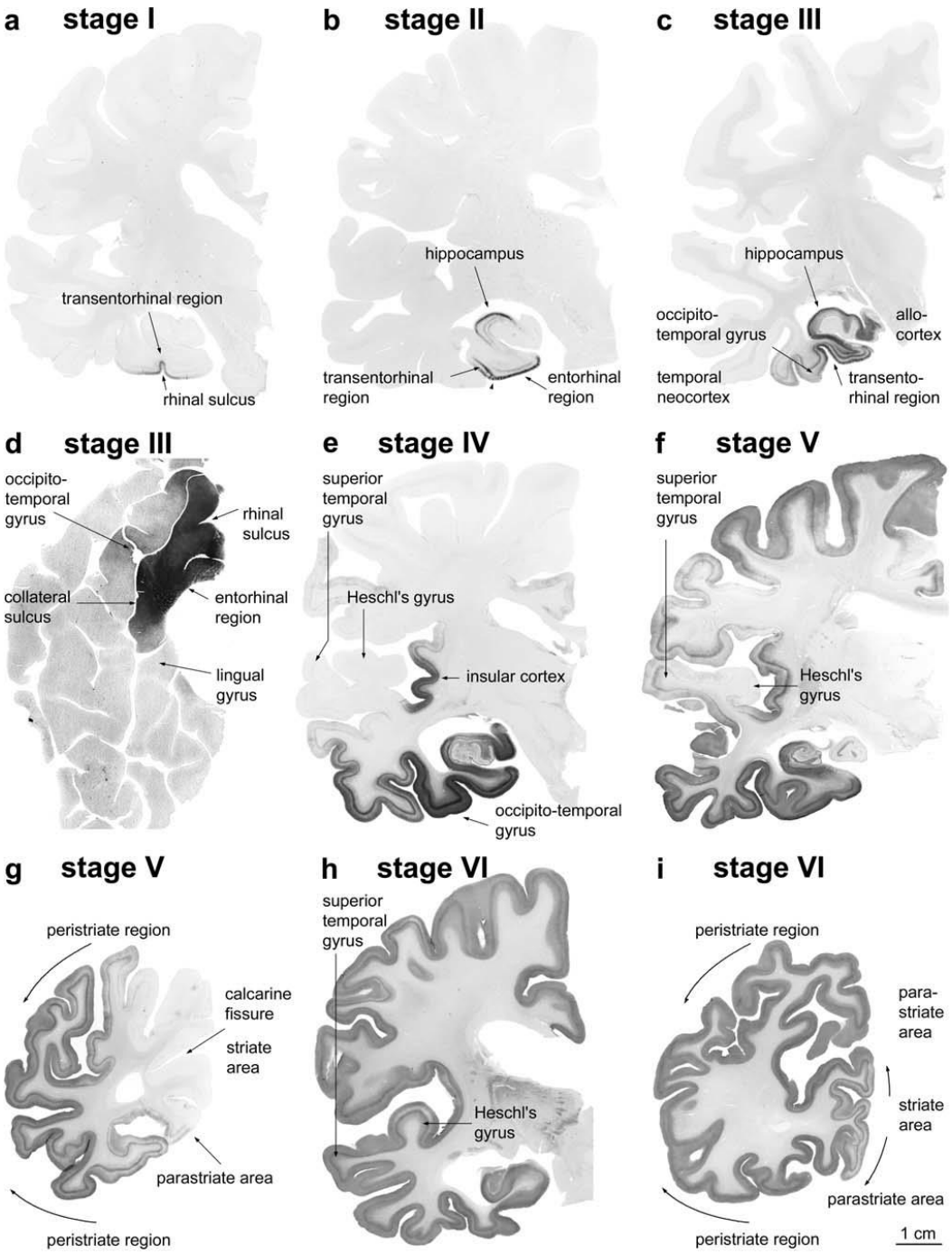

Figure 1. Visualization of the spreading of the Braak stages in human brain (Braak et al., 2006).

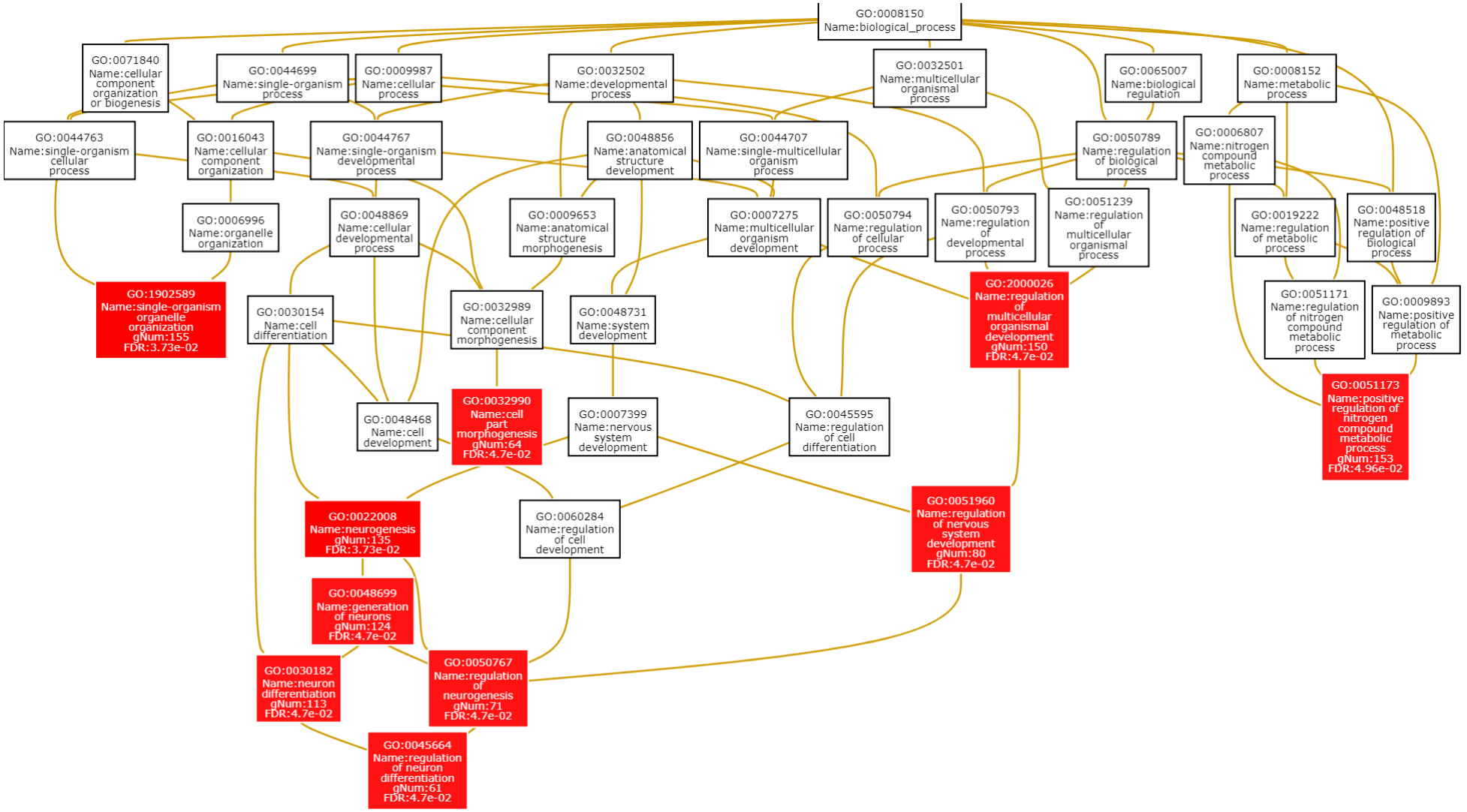

Figure 2. Biological processes of methylation dataset involved in AD (based on Genes.txt)

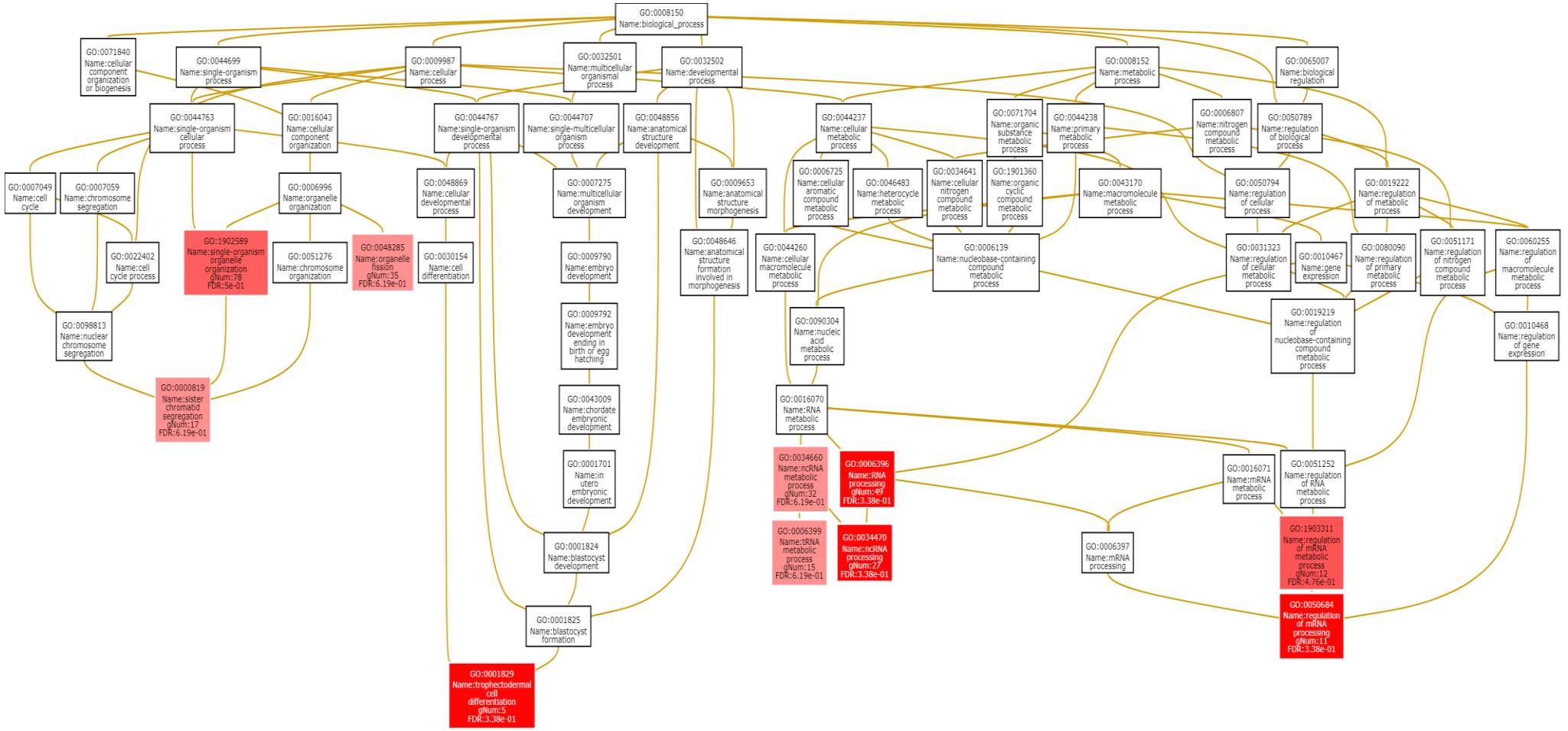

Figure 3. Biological processes of methylation dataset involved in AD (based on Probes.txt).

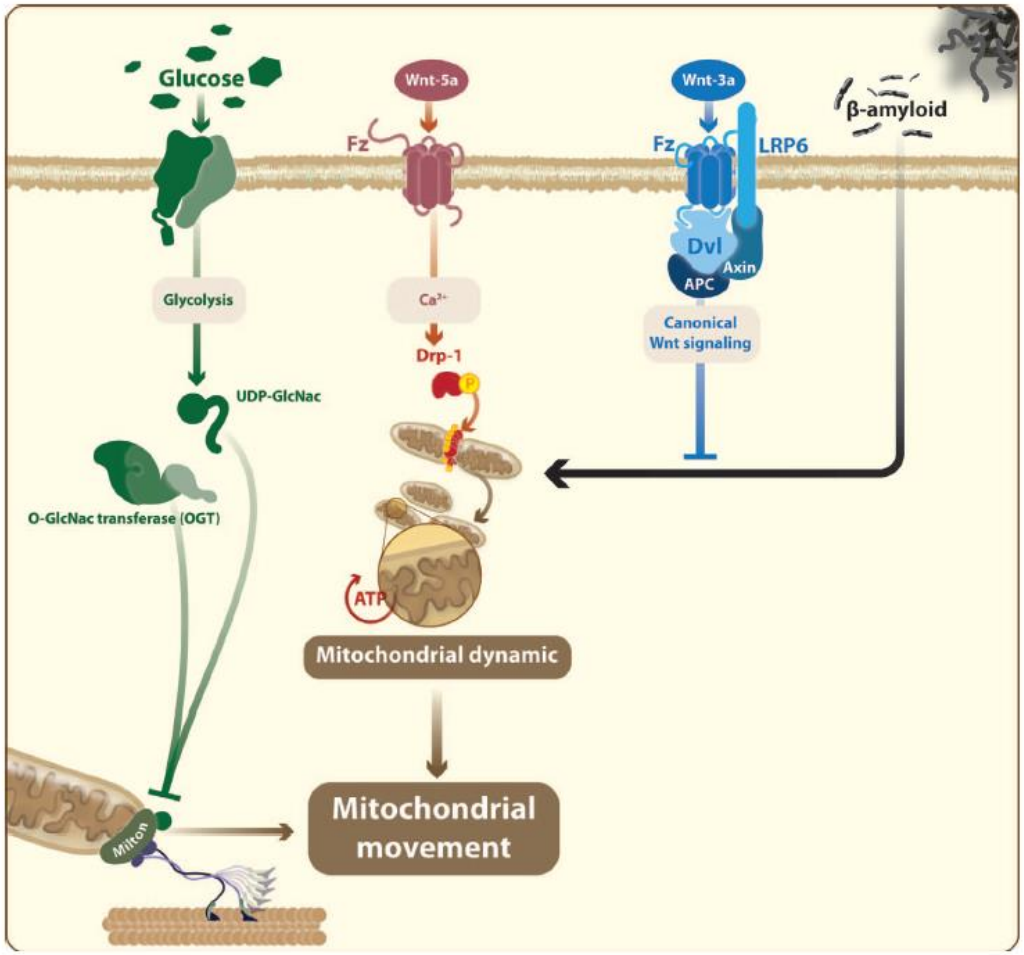

Figure 4. Glucose and Wnt signaling in mitochondrial dynamics (Cisternas & Inestrosa, 2017).

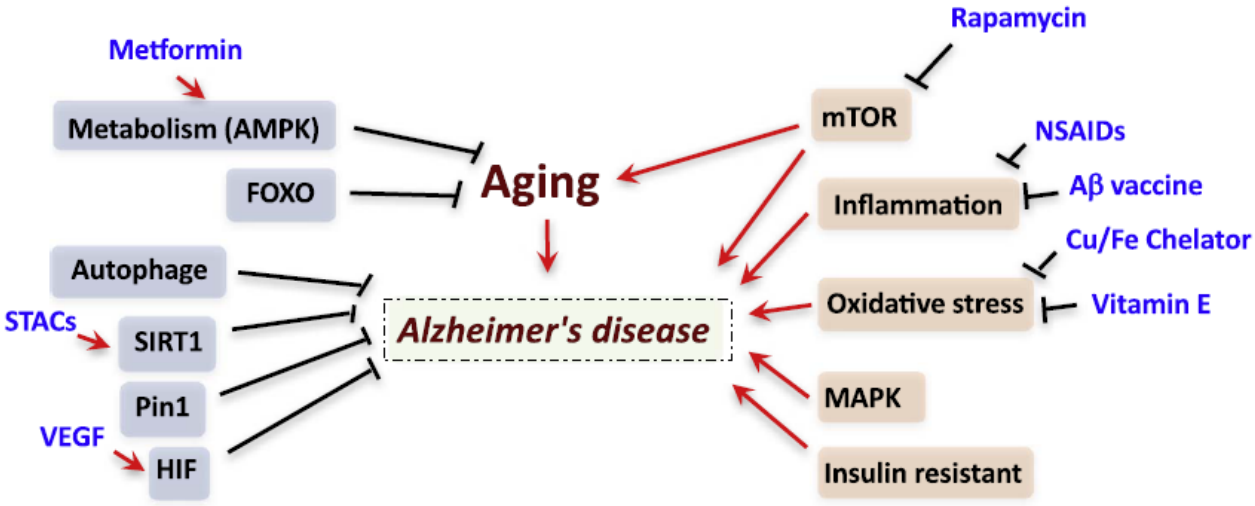

Figure 5. Cancer-related signaling pathways conferring to aging and AD pathogenesis and their potential inhibitors or activators (Guo et al., 2017).

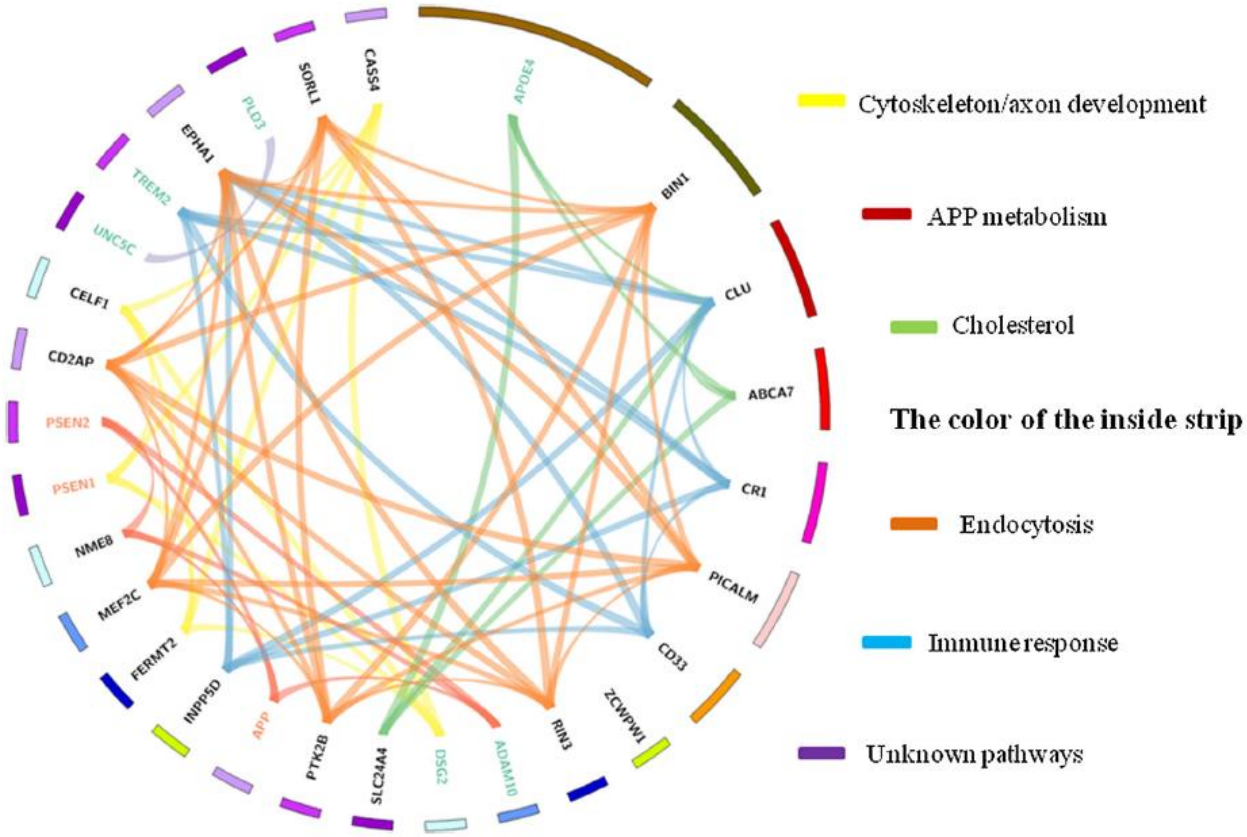

Figure 7. Genes associated with AD (Wang et al., 2019).

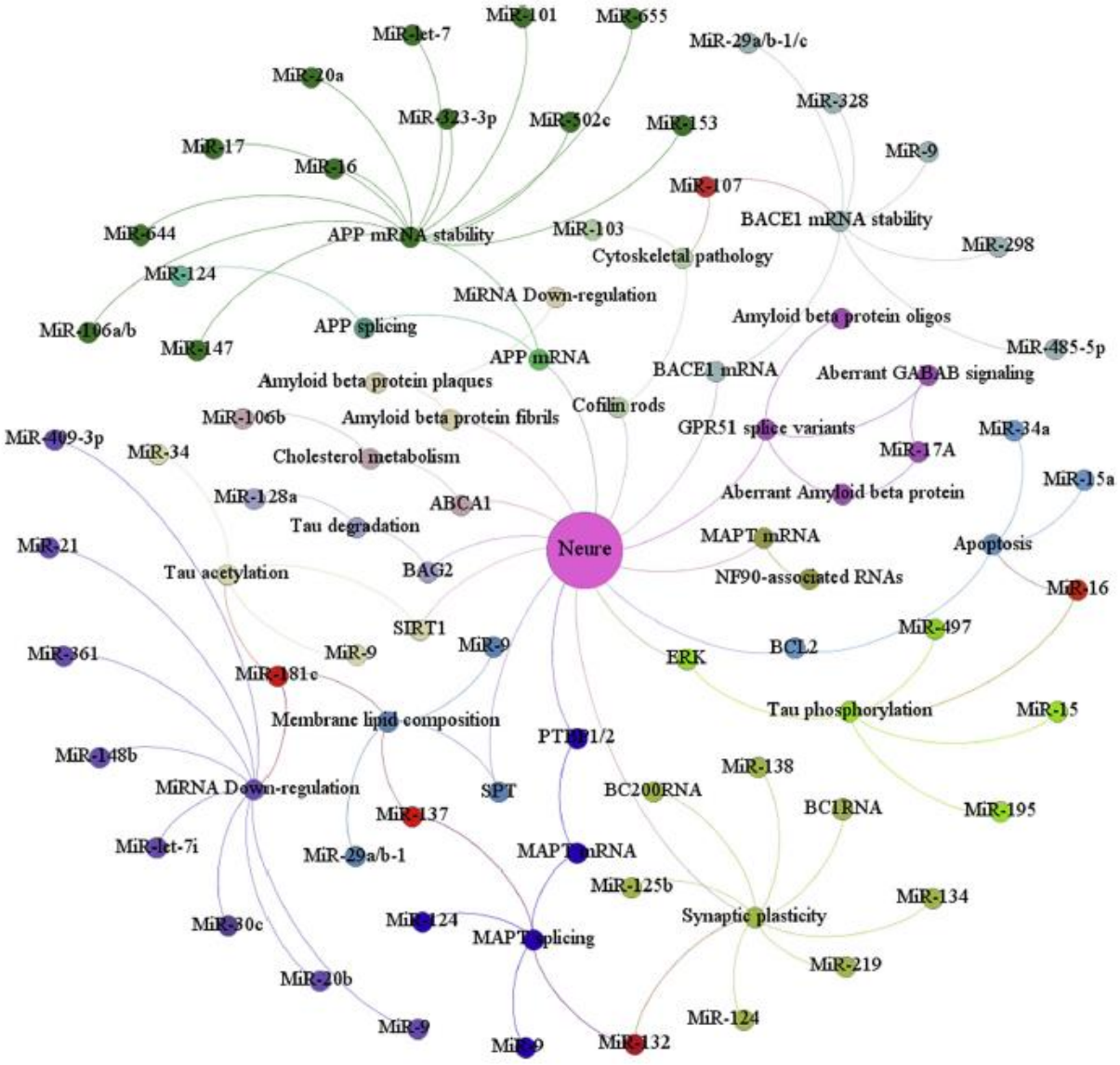

Figure 8. miRNAs associated with AD (Wang et al., 2019).